Structural Differentiation of Diastereomeric Benzo[ghi]fluoranthene Adducts of Deoxyadenosine by Matrix-Assisted Laser Desorption/Ionization Time-of-Flight Mass Spectrometry and Po...

6 AUTHORS, INCLUDING:

Kenneth W Olsen

Loyola University Chicago

71 PUBLICATIONS **2,646** CITATIONS

Damon Barbacci

National Institutes of Health

7 PUBLICATIONS **109** CITATIONS

Structural Differentiation of Diastereomeric Benzo[ghi]fluoranthene Adducts of Deoxyadenosine by Matrix-Assisted Laser Desorption/Ionization Time-of-Flight Mass Spectrometry and Postsource Decay

M. Paul Chiarelli,*,[†] Hui-Fang Chang,[‡] Kenneth W. Olsen,[†] Damon Barbacci,[§] and Bongsup P. Cho[‡]

Department of Chemistry, Loyola University Chicago, Chicago, Illinois 60626, Department of Biomedical Sciences, University of Rhode Island, Kingston, Rhode Island 02881, and Department of Chemistry, Washington University, St. Louis, Missouri 63130

The product ion formation characteristics of four diastereomeric deoxyadenosine adducts formed by the reaction of the syn and anti diastereomers of *trans*-3,4-dihydroxy-5,5a-epoxy-3,4,5,5a-tetrahydrobenzo[ghi]fluoranthene are studied by matrix-assisted laser desorption ionization and postsource decay (PSD) to determine fragmentation pathways that may permit differentiation of their structures. The two adducts derived from each diol-epoxide with DNA differ in structure based on the cis/trans arrangement of the 3′-hydroxyl group on the benzo-[ghi]fluoranthene (B[ghi]F) and the adenine base bound to the B[ghi]F 5a carbon. The two adduct diastereomers with the cis adenine-3′-hydroxyl configuration produce product ions at *m/z* 394 and *m/z* 510 formed by the loss of water that are not observed in the PSD spectra of the two trans isomers. The data suggest a mechanism of water loss that is initiated by a hydrogen-bonding interaction between the charge-bearing proton on the N1 atom and the 3′-hydroxyl oxygen on the polycyclic aromatic hydrocarbon (PAH). Fragmentation is initiated by the transfer of the adenine N1 proton from the nitrogen to the PAH 3′-hydroxyl oxygen and inductive cleavage of the C3−O³ bond to form a benzylic carbocation on B[ghi]F. The proposed mechanism is supported by semiempirical molecular modeling calculations.

Introduction

PAHs[1] are an important class of carcinogens to which human exposure is ubiquitous (*1, 2*). It is believed that these PAHs exert their carcinogenic effects primarily by undergoing metabolic oxidation in route to DNA binding. There are two major pathways through which this metabolic oxidation is thought to occur. The principal pathway involves conversion of the PAH to a diol-epoxide that binds to the primary amine groups on DNA bases (*3, 4*). Another pathway that has been suggested more recently is an enzyme-catalyzed one electron oxidation of the PAH to form a radical cation that may covalently bind to a DNA base and induce depurination (*5*). Studies of the mutagenic potential of B[ghi]F are motivated by the fact that this PAH has been detected at significant levels in urban atmospheres and is known to have a variety of sources (*6*). B[ghi]F may be a good probe of the structure−activity relationships of PAH in mutagenesis as well due to its rigid planar structure. This is because the diol configurations of the diastereomeric anti and syn diol-epoxides formed from this PAH are locked into diequatorial and diaxial orientations, respectively,

thus providing a means of examining the mutagenic potential of adducts in fixed conformations. Earlier studies of the syn and anti diol-epoxides derived from B[ghi]F showed differences in their DNA binding in vitro and in the mutagenicities of the adducts that the diol-epoxides produce when tested in *Salmonella typhimurium* TA 100 (*7, 8*). The study of the structure−activity effects of these B[ghi]F diol-epoxides in vivo will require an analytical methodology that can differentiate the structures of B[ghi]F-DNA adducts at low levels.

Analytical methods based on tandem mass spectrometry may provide a means of detecting DNA adducts with structural information at physiologically important levels. Product ion analyses based on MALDI and ESI have shown promise for differentiating the structures of positional DNA adduct isomers derived from arylamines and PAH at femtomole levels (*9−11*). Differentiating the structures of adducts that are geometric isomers has proven to be more challenging. In several instances, product ion mass spectra acquired as part of the structural characterization of several diol-epoxide and other adducts did not reveal any fragmentation pathways that would permit the differentiation of diastereomers (*12−14*). However, recent product ion studies of cationized tetraols (*15*) and pyrimidine glycols (*16*) suggest that the structural differentiation of diastereomeric PAH DNA adducts should be possible based on the cis/trans arrangement of the hydroxy groups bound to the PAH.

[†] Loyola University Chicago.
[‡] University of Rhode Island.
[§] Washington University.
[1] Abbreviations: PAH, polycyclic aromatic hydrocarbon; B[ghi]F, benzo[ghi]fluoranthene; MALDI, matrix-assisted laser desorption ionization; ESI, electrospray ionization; PSD, postsource decay; dA, deoxyadenosine; T, thymidine; TOFMS, time-of-flight mass spectrometry; PM3, parametric method number 3.
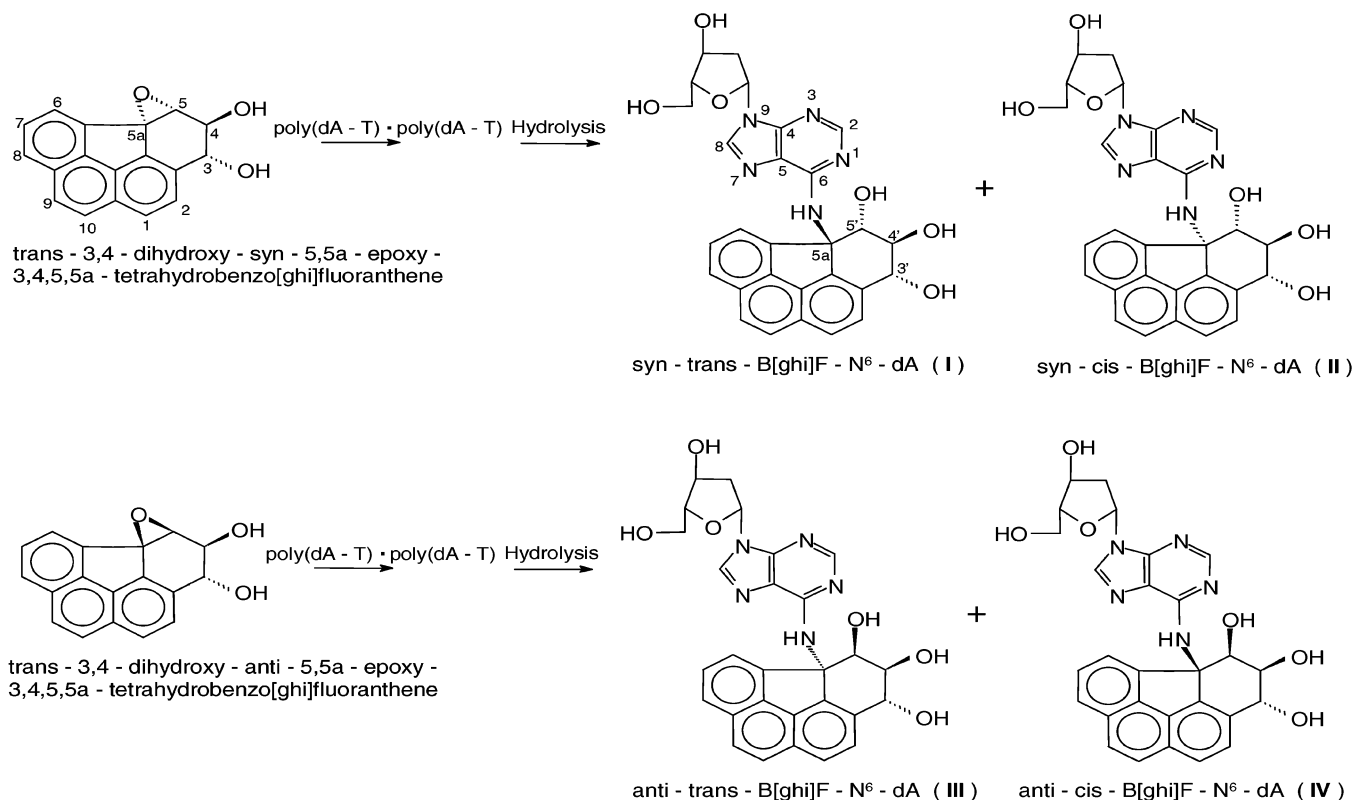
Figure 1. Synthesis, structures, and numbering of the B[ghi]F−C5a−N^6−dA adducts used in this study.

In this study, we examine the fragmentation characteristics of the protonated molecule ions of four B[ghi]F dA adduct diastereomers formed by the reaction of the syn and anti diastereomers of *trans*-3,4-dihydroxy-5,5a-epoxy-3,4,5,5a-tetrahydrobenzo[ghi]fluoranthene with DNA and poly(dA-T)·poly(dA-T) and calf-thymus DNA. The reaction of each diol-epoxide produces two adducts that differ in structure based on cis/trans arrangement of the hydroxyl group and adenine base bound to the C3 and C5a carbons of B[ghi]F, respectively (Figure 1). dA adducts with the cis structural configuration form significant abundances of product ions produced by the loss of water upon collisional activation. Molecular orbital calculations suggest that the loss of water occurs through an intermediate where the charge-bearing proton on the N1 nitrogen of adenine is hydrogen-bonded to the B[ghi]F 3′-hydroxyl oxygen. This bond cleavage occurs at the C3 position of the B[ghi]F predominantly because of the stability of the incipient carbocation. These results suggest that the structures of diastereomeric dA adducts produced by either the syn or the anti diol-epoxide of B[ghi]F might be recognized when conducting DNA binding studies in a rodent model.

Materials and Methods

Caution: *anti- and syn-B[ghi]F diol-epoxides are potentially carcinogenic chemicals and should be handled carefully in accordance with NIH guidelines.*

Sample Preparation. The B[ghi]F-derived dA adducts syn-trans (**I**), syn-cis (**II**), anti-trans (**III**), and anti-cis (**IV**) B[ghi]-F-5a-N^6-dA used in this study were synthesized by the reaction of anti- and syn-B[ghi]F diol-epoxides with poly(dA-dT)·poly-(dA-dT). The structures of these adducts and their diol-epoxide precursors are shown in Figure 1. The synthesis and structural characterization of these adducts (*7, 8*) and their precursor diol-epoxides (*17*) are described elsewhere.

Mass Spectrometry. MALDI PSD spectra were acquired with a PerSeptive Biosystems, Inc. Voyager DE-RP mass spectrometer (Framingham, MA) at the Washington University Resource for Biomedical and Bio-organic Mass Spectrometry in St. Louis, MO. The instrument was operated in the continuous ion extraction mode with a total acceleration potential of 25 kV. A nitrogen laser (337 nm, 20 kW peak laser power, 5 ns pulse width) was used to induce desorption and ionization. All spectra were acquired in the positive ion mode. The B[ghi]F-dA adducts used in this study were dissolved in methanol to give final concentrations of approximately 4 pm μL^{-1}. α-Cyano-4-hydroxy-cinnamic acid was used as the matrix. The matrix was prepared as a 1 mg/mL solution in 2:1 CH$_3$CN:H$_2$O that was 0.1% in trifluoroacetic acid. The adduct and matrix solutions were combined to give a matrix:analyte molar ratio of 5 × 10^3. The absolute quantity of analyte applied to the laser probe in the individual sample preparations was approximately 2 pm for the purpose of comparing product ion spectra. The samples were allowed to dry under ambient conditions before introduction into the mass spectrometer. Normally, 20−30 laser shots were averaged to produce a PSD spectrum. Four 20−30 laser shot spectra were acquired from each sample preparation.

PSD spectra were acquired by filling the collision cell with argon to a pressure of 2 × 10^{-6} Torr. The *m/z* 528 ion was selected in all product ion analyses. The resolution with which precursor ions could be selected for product ion analysis was approximately 25−50. The background signal level was determined by analyzing the matrix alone in the same mass window-(s) in which the protonated molecule ions were selected for PSD analysis. A minimum of two sample preparations was analyzed for the purpose of comparing abundances of product ions formed by the fragmentation of the B[ghi]F-dA adducts. Raw data were acquired with a Tektronix TDS 520A oscilloscope and subsequently transferred to a PC for data processing.

Molecular Modeling. Molecular modeling was used to find the minimum energy conformations for the protonated adducts in the gas phase and the corresponding carbocations produced after the loss of water. The models were built using Spartan 5.0 (Wave function, Irvine, CA), and the initial geometry was
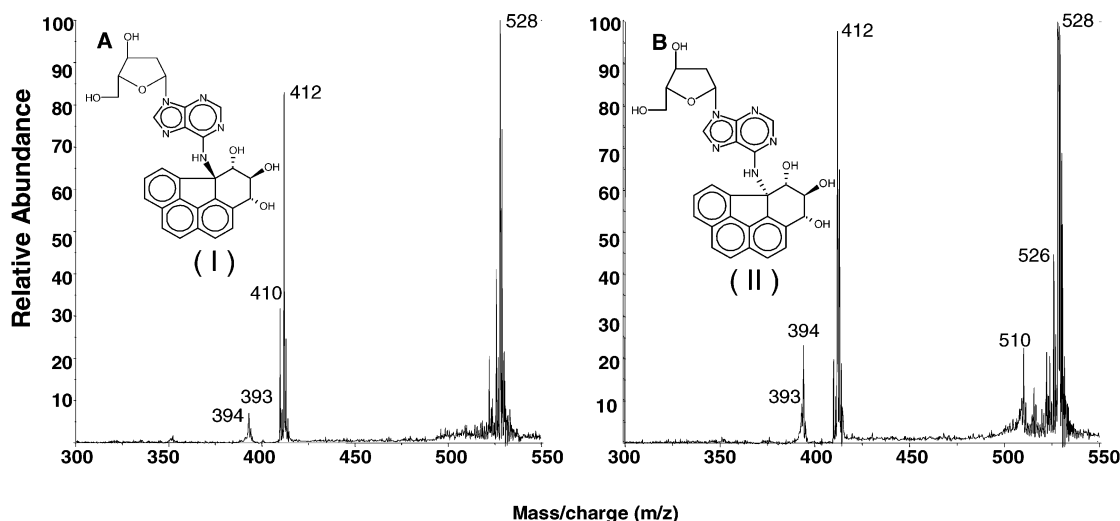
Figure 2. MALDI−PSD product ion spectra of the protonated molecule ion at m/z 528 derived from (A) *syn−trans−*B[ghi]F−N[6]−dA (**I**) and (B) *syn−cis−*B[ghi]F−N[6]−dA (**II**), the dA adducts formed by the reaction of *trans-*3,4-dihydroxy-*syn-*5,5a-epoxy-3,4,5,-5a-tetrahydrobenzo[ghi]fluoranthene with poly(dA-T)·poly(dA-T).

optimized using the PM3 semiempirical method as implemented in Spartan. Calculations were carried out assuming that charge-bearing proton was attached to the N1 nitrogen of the adenine ring. Starting with this optimized structure for each protonated adduct, a conformational search was done by rotating about the two conformational sensitive bonds on either side of the nitrogen (N[6]) bridging the adenine and the PAH. The 36 conformations generated for each structure were geometry-optimized using PM3, and the final energies were compared. The carbocation structures were generated by maintaining the most stable adduct conformations after removing water. Single point energies were calculated using the PM3 method for each carbocation and compared.

Results and Discussion

Fragmentation Characteristics of B[ghi]F-dA Adducts. These product ion studies were undertaken to find a tandem MS method that permitted the differentiation of diastereomeric B[ghi]F-dA adducts. This investigation was motivated by earlier PSD studies of B[ghi]F tetrol diastereomers in which tetrol structures were differentiated through the PSD product ion analysis of (M + Li)+ ions. The tetrol product ion studies suggested that the proportion of fragment ions formed by water loss was determined by the cis/trans arrangement of four hydroxy groups about the aliphatic carbons 3, 4, 5, and 5a. These four dA-B[ghi]F adduct structures are different based on the cis/trans arrangement of the three hydroxyl groups and adenine base about carbons 3, 4, 5, and 5a (Figure 1). Therefore, we believed that these adduct structures might be differentiated through similar water loss fragmentation pathways. Analysis of the (M + Li)+ ions formed from these dA adducts did not show any fragments formed by the loss of water, however. PSD product ion spectra of the protonated molecule ions derived from these adducts acquired during the initial structural characterization studies did not show any fragmentation pathways that would differentiate diastereomers. The only adduct to show any evidence for loss of water was *anti-trans-*B[ghi]F-N[6]-dA (**III**), which formed an ion at m/z 394, corresponding to loss of the deoxyribose and water (7).

In the next set of experiments, we tried to increase the amount of fragmentation observed in the PSD spectra of

these dA adducts by increasing the number of collisions the protonated molecule ions undergo after exiting the source of the TOFMS. Therefore, the collision cell was filled with argon to a pressure of 2×10^{-6} Torr. Two adducts, *syn-cis-*B[ghi]F-N[6]-dA (**II**) and **III**, both produce significant abundances of two ions formed by the loss of water not observed in the PSD spectra of adducts **I** and **IV**. The protonated molecule ions generated from adducts **II** and **III** yield ions at m/z 394 (fragmentation is described above) and at m/z 510, which involves loss of water from the protonated molecule ion at m/z 528 directly. Partial PSD product ion mass spectra of the protonated molecule ions generated from these adducts highlighting the mass range where water loss ions are observed are shown in Figures 2 and 3. The ions observed at m/z 393 and m/z 509 may be derived from a molecule radical cation formed by photoionization of the B[ghi]F ring system by the laser. The other fragmentation pathways observed here are consistent with those described previously (*3, 18, 19*) and do not appear to be indicative of the geometric isomerism of these compounds. The average relative abundances of all product ions observed in these determinations are summarized in Table 1. The ions at m/z 136 and m/z 252 are the protonated adenine and dA ions, respectively. The ions at m/z 277, m/z 259, and m/z 231 are formed from bond cleavages in the trihydroxy B[ghi]F group.

Each of the diol-epoxides (shown in Figure 1) should, upon reaction with DNA, produce one dA adduct that undergoes loss of water and one adduct that does not during product ion analysis. The differences in fragmentation suggest that the structures of DNA adducts formed by a particular diol-epoxide diastereomer in a laboratory animal during metabolism studies may be differentiated without the use of standard compounds for comparison. The following discussion is concerned with understanding the mechanism of water loss that permits the structural differentiation of dA adducts formed from diol-epoxide of known structure.

Mechanism of Water Loss. The two adducts that form significant abundances of fragment ions formed by water loss are **II** and **III**. The one structural feature that differentiates these two from the other dA adducts is that
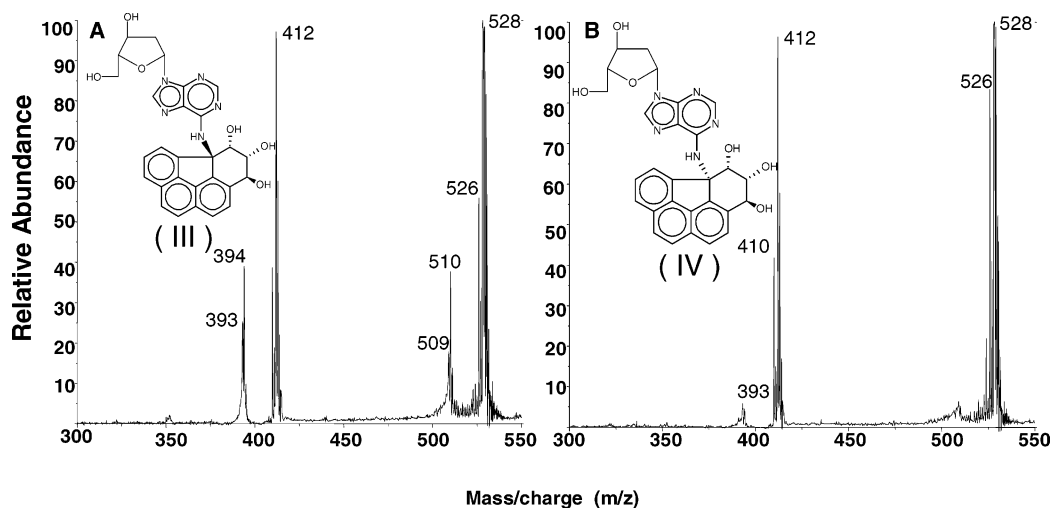
Figure 3. MALDI−PSD product ion spectra of the protonated molecule ion at *m/z* 528 derived from (A) *anti-trans*-B[ghi]F-N[6]-dA (**III**) and (B) *anti-cis*-B[ghi]F-N[6]-dA (**IV**), the dA adducts formed by the reaction of *trans*-3,4-dihydroxy-*anti*-5,5a-epoxy-3,4,5,5a-tetrahydrobenzo[ghi]fluoranthene with poly(dA-dT)·poly(dA-dT).

Table 1. Average Relative Abundances (*n* = 8) of the Product Ions Formed in the PSD Analysis of the Protonated Molecule Ion at *m/z* 528 for the Four Diastereomeric B[ghi]F-N[6]-dA Adducts Used in This Study[a]

m/z	syn-trans (**I**)	syn-cis (**II**)	anti-trans (**III**)	anti-cis (**IV**)
510	4 ± 4	16 ± 5	35 ± 9	0
394	3 ± 2	15 ± 6	30 ± 6	2 ± 1
277	1 ± 1	4 ± 2	4 ± 1	4 ± 1
259	1 ± 1	5 ± 2	6 ± 1	7 ± 2
252	35 ± 5	31 ± 11	46 ± 9	23 ± 3
231	7 ± 1	18 ± 6	11 ± 2	11 ± 2
136	8 ± 1	8 ± 3	14 ± 4	7 ± 1

[a] The ion at *m/z* 412 is the base peak (100% RA) in all spectra acquired.

the 3′-hydroxyl group and the adenine base are cis with respect to each other. This suggests that a hydrogen-bonding interaction between the 3′-hydroxyl group and the adenine base plays a role in the formation of the fragment ions observed at *m/z* 394 and *m/z* 510. The structures of all four adducts suggest that hydrogen-bonding between one of the protonated adenine nitrogens and the hydroxyl oxygens of B[ghi]F may be feasible when the base and the hydroxyl groups are cis with respect to each other. If such a hydrogen-bonding interaction exists prior to collisional activation, then water loss might proceed through the transfer of a proton to the 3′-hydroxyl oxygen and an inductive cleavage (*20*) of the C3′−O3′ bond to form a carbocation at the B[ghi]F C3′ carbon. This proposed mechanism is summarized in Figure 4.

We carried out semiempirical molecular modeling calculations of the adenine adduct protonated molecule ions to determine if such hydrogen-bonding interactions between the base and the B[ghi]F hydroxyl oxygens were possible. Minimum energy configurations were calculated from 36 different initial conformations for each of the N1 protonated molecule ions (vide supra). The N1 nitrogen was assumed to be the charge site that initiates water loss because molecular orbital calculations suggest that the proton affinity of the adenine N1 nitrogen is greater than the N7 nitrogen by 9 kcal/mol (*20*). The N3 nitrogen is too far from the B[ghi]F hydroxyl oxygens for hydrogen bonding to occur as well.

The initial configurations were arrived at by rotating the positions of the adenine base and B[ghi]F group about the adenine C6−N[6] bond and the adenine N[6]−B[ghi]-F−C5a bond in 60° intervals. In many instances, different starting configurations converged at the same minimum energy structures.

The results of these calculations suggest that minimum energy structures involving hydrogen bonds between the charge-bearing proton on either adenine nitrogen or B[ghi]F hydroxyl oxygens are possible with each of the three hydroxy groups on the B[ghi]F, but only when a hydroxy group and adenine are cis with respect to each other. A model of such a hydrogen-bound structure is shown in Figure 5. Two other types of structures corresponding to energy minima were encountered in these calculations. One is characterized by the interaction of the charge-bearing proton on the N1 nitrogen with the π-cloud of the B[ghi]F ring system. The other minimum energy structure has the charge-bearing proton protruding away from the center of the adduct molecule and not involved in any hydrogen-bonding interactions with other functional groups.

Another important aspect of this mechanism is the stability of the carbocation formed after the loss of water. Molecular orbital calculations indicate that the carbocation formation at the B[ghi]F−C3 benzylic carbon (after loss of the protonated hydroxyl group) is favored over carbocation formation at C4 and C5 positions of the B[ghi]F by ca. 25 kcal/mol. Therefore, inductive cleavage of the C3−O[3] bond should proceed more readily than the cleavage of the C4−O[4] or C5−O[5] bonds. The results of all of the molecular mechanics calculations are summarized in Table 2. The results of the molecular modeling calculations support a mechanism of water loss (illustrated in Figure 4) initiated by a hydrogen-bonding interaction between the charge-bearing proton on the N1 nitrogen of adenine.

Conclusion

The product ion formation characteristics of four B[ghi]F-5a-N[6]-dA diastereomers have been studied using MALDI and PSD to determine fragmentation pathways that may be used to differentiate the structures of these
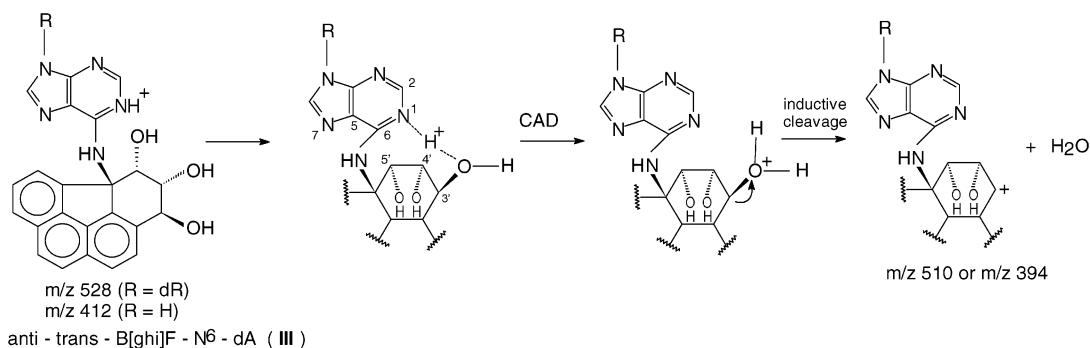
Figure 4. Proposed mechanism of water loss from the protonated molecule ions (m/z 528) and BH_2^+ ions (m/z 412) derived from the B[ghi]F-C5a-N^6-dA adducts used in this study.
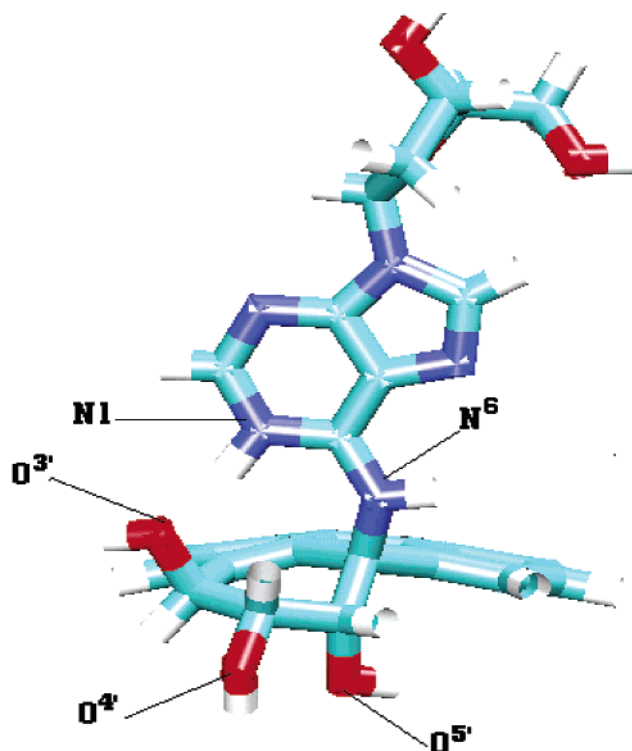

Figure 5. Optimized minimum energy structure of *anti-trans*-B[ghi]F-N^6-dA (**III**) containing a hydrogen bond between the adenine N1 nitrogen and the B[ghi]F O^3 oxygen.

Table 2. Heats of Formation (kcal/mol) of Adenine N1-B[ghi]F Hydroxyl Oxygen, Hydrogen-Bonded Intermediates, and Carbocations Formed in the Fragmentation of the dA-N^6-C5a-B[ghi]F Adducts

DNA adduct	hydroxyl oxygen bound to adenine N1 proton	ΔH_f of hydrogen-bonded intermediate	ΔH_f of carbocation formed during water loss
syn-trans (**I**)	$O^{4'}$	33.09	199.9
	$O^{4'}$	43.26	189.6
syn-cis (**II**)	$O^{3'}$	30.18	162.7
	$O^{3'}$	31.03	164.2
	$O^{5'}$	26.98	185.2
	$O^{5'}$	27.1	185.1
	$O^{5'}$	28.8	185.2
anti-trans (**III**)	$O^{3'}$	31.11	163.8
	$O^{3'}$	63.88	159.1
anti-cis (**IV**)	$O^{4'}$	35.09	195.0
	$O^{5'}$	30.82	196.1

adducts when detected in vivo. The reaction of each diol-epoxide produces two adducts that differ in structure based on the cis/trans arrangement of the hydroxyl group

and adenine base bound to the C3 and C5a carbons of B[ghi]F. Those adducts that have a cis 3′-hydroxyl adenine configuration form significant abundances of ions at m/z 394 and m/z 510 due to the loss of water. These structural features are consistent with a mechanism of water loss that is initiated by a hydrogen-bonding interaction between the charge-bearing proton on the adenine N1 nitrogen and the 3′-hydroxyl oxygen on the B[ghi]F group. Fragmentation occurs after the transfer of the charge-bearing proton to the 3′-hydroxyl oxygen by inductive cleavage of the C3–O^3 bond to produce a benzylic carbocation on the B[ghi]F. The proposed mechanism is supported by semiempirical molecular modeling calculations. The results of this study suggest that the structures of adducts, produced by the metabolism of a PAH diol-epoxide in a laboratory animal, may be differentiated when detected without the use of standard compounds.

References

(1) Harvey, R. G. (1996) Mechanisms of carcinogenesis of polycyclic aromatic hydrocarbons. *Polycyclic Aromat. Compd.* **9**, 1–23.

(2) Conney, A. H. (1982) Induction of microsomal enzymes by foreign chemicals and carcinogenesis by polycyclic aromatic hydrocarbons: G. H. A. Clowes Memorial Lecture. *Cancer Res.* **42**, 4875–4917.

(3) Dipple, A., Khan, Q. A., Page, J. E., Ponten, I., and Szeliga, J. (1999) DNA reactions, mutagenic action and stealth properties of polycyclic aromatic hydrocarbon carcinogens (Review). *Int. J. Oncol.* **14**, 103–111.

(4) Beland, F. A., and Poirier, M. C. (1989) DNA adducts and carcinogenesis. In *The Pathobiology of Neoplasia* (Sirica, A. E., Ed.) pp 57–80, Plenum, New York.

(5) Cavalieri, E. L., and Rogan, E. G. (1992) The approach to understanding aromatic hydrocarbon carcinogenesis. The central role of radical cations in metabolic activation. *Pharmacol. Ther.* **55**, 83–199.

(6) Harvey, R. G. (1991) *Polycyclic Aromatic Hydrocarbons: Chemistry and Carcinogenecity*; Cambridge University Press: Cambridge, United Kingdom.

(7) Chang, H.-F., Huffer, D. M., Chiarelli, M. P., and Cho, B. P. (2002) Characterization of DNA adducts and tetraols derived from anti-benzo[ghi]fluoranthene-3,4-dihydrodiol-5,5a-epoxide. *Chem Res. Toxicol.* **15**, 187–197.

(8) Chang, H.-F., Huffer, D. M., Chiarelli, M. P., Blankenship, L. R., Culp, S. J., and Cho, B. P. (2002) Characterization of DNA adducts derived from syn-benzo[ghi]fluoranthene-3,4-dihydrodiol-5,5a-epoxide and comparative DNA binding studies with structurally related anti-diol-epoxides of benzo[ghi]fluoranthene and benzo[c]phenanthrene. *Chem. Res. Toxicol.* **15**, 198–208.

(9) Cavalieri, E. L., Stack, D. E., Devanesan, P. D., Todorovic, R., Dwivedy, I., Higginbotham, S., Johansson, S. L., Patil, K. D., Gross, M. L., Gooden, J. K., Ramanathan, R., Cerny, R. L., and Rogan, E. G. (1997) Molecular origin of cancer: catechol estrogen-3,4-quinones as endogenous tumor initiators. *Proc. Natl. Acad. Sci. U.S.A.* **94**, 10937−10942.

(10) Harsch, A., Sayer, J. M., Jerina, D. M., and Vouros, P. (2000) HPLC-MS/MS identification of positionally isomeric benzo[*c*]-phenanthrene diol-epoxide adducts in duplex DNA. *Chem. Res. Toxicol.* **13**, 1342−1348.

(11) Embrechts, J., Lemiere, F., Van Dongen, W., and Esmans, E. L. (2001) Equilenin-2′-deoxynucleoside adducts: analysis with nano-liquid chromatography coupled to nano-electrospray tandem mass spectrometry. *J. Mass Spectrom.* **36**, 317−328.

(12) Li, K. M., George, M., Gross, M. L., Lin, C. H., Jankowiak, R., Small, G. J., Seidel, A., Kroth, H., Rogan, E. G., and Cavalieri, E. L. (1999) Structure elucidation of the adducts formed by the fjord region dibenzo[a,l]pyrene-11,12-dihydrodiol 13,14-epoxides with deoxyguanosine. *Chem Res. Toxicol.* **12**, 778−788.

(13) Li, K. M., George, M., Gross, M. L., Seidel, A., Luch, A., Rogan, E. G., and Cavalieri, E. L. (1999) Structure elucidation of the adducts formed by the fjord region dibenzo[a,l]pyrene-11,12-dihydrodiol 13,14-epoxides and deoxyadenosine. *Chem. Res. Toxicol.* **12**, 758−767.

(14) Wang, M., McIntee, E. J., Cheng, G., Shi, Y., Villalta, P. W., and Hecht, S. S. (2000) Identification of paraldol-deoxyguanosine adducts in DNA reacted with crotonaldehyde. *Chem. Res. Toxicol.* **13**, 1065−1074.

(15) Huffer, D. M., Chang, H.-F., Cho, B. P., Zhang, L., and Chiarelli, M. P. (2001) Product ion studies of diastereomeric benzo[ghi]-fluoranthene tetraols by matrix-assisted laser desorption ionization time-of-flight mass spectrometry and post-source decay. *J. Am. Soc. Mass Spectrom.* **12**, 376−378.

(16) Wang, Y., Vivekananda, S., and Zhang, K. (2002) ESI-MS/MS for the differentiation of diastereomeric pyrimidine glycols in mono-nucleosides. *Anal. Chem.* **74**, 4505−4512.

(17) Branco, P. S., Chiarelli, M. P., Lay, J. O., Jr., and Beland, F. A. (1995) Low energy tandem mass spectrometry of deoxynucleoside adducts of polycyclic aromatic hydrocarbon dihydrodiol-epoxides. *J. Am. Soc. Mass Spectrom.* **6**, 248−256.

(18) Stemmler, E. A., Buchanan, M. V., Hurst, G. B., and Hettich, R. L. (1994) Structural characterization of polycyclic aromatic hydrocarbon dihydrodiol epoxide DNA adducts using matrix-assisted laser desorption/ionization Fourier transform mass spectrometry. *Anal. Chem.* **66**, 1274−1285.

(19) McLafferty, F. W., and Tureček (1993) *Intrepretation of Mass Spectra*, pp 64−67, University Science Books, Mill Valley, CA.

(20) Del Bene, J. E. (1983) Molecular orbital study of the protonation of DNA bases. *J. Phys. Chem.* **87**, 367−372.